

A bis(3-hydroxy-4-pyridinone)-EDTA derivative as a strong chelator for M^{3+} hard metal ions: complexation ability and selectivity†

Sofia Gama,^{a,b} Paul Dron,^a Silvia Chaves,^a Etelka Farkas^c and M. Amélia Santos^{*a}

Received 11th March 2009, Accepted 30th April 2009

First published as an Advance Article on the web 9th June 2009

DOI: 10.1039/b904950a

The study of chelating compounds is very important to solve problems related to human metal overload. 3-Hydroxy-3-pyridinones (HP), namely deferiprone, have been clinically used for chelating therapy of Fe and Al over the last decade. A multi-disciplinary search for alternative molecules led us to develop poly-(3-hydroxy-4-pyridinones) to increase metal chelation efficacy. We present herein a complexation study of a new bis-(3-hydroxy-4-pyridinone)-EDTA derivative with a set of M^{3+} hard metal ions ($M = \text{Fe, Al, Ga}$), as well as Zn^{2+} , a biologically relevant metal ion. Thus a systematic aqueous solution equilibrium study was performed using potentiometric and spectroscopic techniques (UV-Vis, NMR methods). These set of results enables the establishment of specific models as well as the determination of thermodynamic stability constants and coordination modes of the metal complexes. The results indicate that this ligand has a higher affinity for chelating to these hard metal ions than deferiprone, and that the coordination occurs mostly through the HP moieties. Furthermore, it was also found that this ligand has a higher selectivity for chelating to M^{3+} hard metal ions ($M = \text{Fe, Al, Ga}$) than Zn^{2+} .

1. Introduction

The development of chelating agents for the mobilization of excess hard metal ions has been the object of research interest,^{1,2} either due to high body metal burden owed to metabolic defects of endogenous metals (e.g. Fe^{3+}) or to exogenous metal ion intoxication (e.g. Al^{3+}). In fact, although iron is an essential element in life, there are many conditions of iron overload (transfusional iron overload and hemochromatosis), which can result in iron related toxicity and damage to several organs.³ On the other hand, aluminium accumulation in some organs can be highly toxic, namely in the brain (dialysis encephalopathy) and also in the bones (osteomalacia).⁴⁻⁶

Desferrioxamine B (DFO) is a naturally occurring trihydroxamic acid which has been used for decades as a chelating agent for the treatment of patients with transfusional iron overload. However, the drawbacks associated with this therapy, such as high cost and low patient compliance associated with its subcutaneous (s.c.) or intravenous (i.v.) daily administration over

several hours, led to the investigation for new chelating drugs.⁷ Major advances in the development of new chelators appeared in the 3-hydroxypyridin-4-one (3,4-HP) family of compounds, namely after the disclosure (ca. 15 years ago) of deferiprone (DFP, 1,2-dimethyl-3-hydroxypyridin-4-one) as an orally active drug for the treatment of transfusional iron overload.⁸ This family of compounds can be easily made and *N*-functionalized to allow for the tuning of important physicochemical properties which enable the selectivity of the biodistribution at different organs (without disturbing the metal-binding efficacy). A large number of extra functionalized mono-3,4-HPs have been recently developed.⁹⁻¹¹ However, since they are bidentate ligands, their efficacy as chelating agents requires quite high molar doses to fulfil the coordination to these three charged metal ions.

To overcome the dilution problem and improve the chelating efficiency, a number of polydentate ligands have been developed by different research groups including ours, namely tris-3,4-HP;^{12,13} and also bis-3,4-HP derivatives, having two binding units appended to amino acid skeletons (imino-diacetic acid), to be used alone¹⁴ or in combination with other mono-3,4-HPs in order to increase the chelating efficacy.^{15,16} Herein, we present new results associated with a metal complexation study of another polydentate derivative having two 3,4-HP binding units attached to ethylenediaminetetraacetic acid (EDTA), while the extra pair of carboxylic groups could be thought as for eventual metal extra-coordination or to enable the interaction with bio-sites (*per se* or upon extra functionalization). Although this compound ($\text{EDTAPr}(3,4\text{-HP})_2$) has already been previously bioassayed,¹⁷ we describe herein further studies on the complexation of this derivative with iron(III) and aluminium(III) in aqueous solution in view of its potential application as a sequestering agent for these metal ions, and also the analogous studies with gallium(III) taking into account its use as a radiotracer model for Fe- or

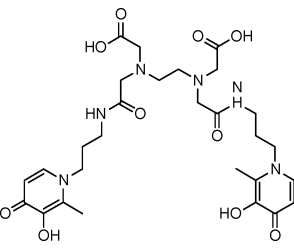
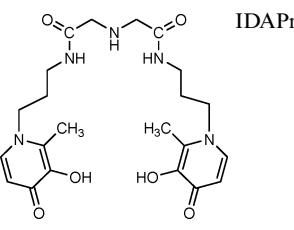
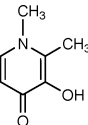
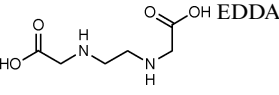
^aCentro de Química Estrutural, Complexo I, Instituto Superior Técnico, 1049-001 Lisboa, Portugal. E-mail: masantos@ist.utl.pt

^bInstituto Tecnológico e Nuclear, Estrada Nacional No 10, 2686-953 Sacavém, Portugal

^cDepartment of Inorganic and Analytical Chemistry, University of Debrecen, H-4010 Debrecen, Hungary

† Electronic supplementary information (ESI) available: Fig. S1: potentiometric titration curves obtained for the different EDDA-M(III) systems ($M = \text{Fe, Al, Ga}$); Fig. S2: absorption spectra registered at different pH values for the $\text{EDTAPr}(3,4\text{-HP})_2\text{-Fe(III)}$ system; Fig. S3: graphical representation of the chemical shifts as a function of pD of the spectra obtained for the ligand $\text{EDTAPr}(3,4\text{-HP})_2$ and the $\text{EDTAPr}(3,4\text{-HP})_2\text{-Al(III)}$ system; Fig. S4: potentiometric titration curves of aqueous solutions containing $\text{EDTAPr}(3,4\text{-HP})_2$ alone, and in the presence of Zn^{2+} ; Fig. S5: ¹H NMR spectra of the ligand $\text{EDTAPr}(3,4\text{-HP})_2$ and in the presence of Zn(II) . See DOI: 10.1039/b904950a

Table 1 Stepwise protonation constants ($\log K_i$) for EDTAPr(3,4-HP)₂, IDAPr(3,4-HP)₂, 3,4-DMHP and EDDA ligands, as well as the cumulative formation constants ($\log \beta$) for their metal(III) complexes (M = Fe, Ga, Al), at $I = 0.2$ M KCl and $T = 25.0 \pm 0.1$ °C; pM values^a for these compounds and some other relevant synthetic and biological ligands

Ligands	$\log K_i$	Complex $M_pH_qL_r$ (p,q,r)	$\log \beta$				
			$Fe_pH_qL_r$	$Ga_pH_qL_r$	$Al_pH_qL_r$	$Zn_pH_qL_r$	
 EDTAPr(3,4-HP) ₂		(1,-1,1)	22.87(4)	—	15.2(3)	—	
		(2,3,3)	95.1(3)	—	81.2(2)	—	
		(2,2,3)	89.6(9)	86.53(4)	—	—	
		(2,1,3)	82.4(9)	81.22(6)	68.1(5)	—	
		(2,0,3)	73.6(9)	71.82(9)	60.6(6)	—	
		(1,4,1)	40.09(4)	38.6(1)	35.1(2)	36.31(3)	
		(1,3,1)	38.43(4)	37.19(7)	33.0(1)	33.44(2)	
		(1,2,1)	37.15(5)	34.22(7)	30.62(9)	29.45(3)	
		(1,1,1)	34.19(4)	30.7(1)	27.58(7)	21.18(4)	
		(1,0,1)	29.62(4)	—	—	11.34(4)	
		(2,1,1)	—	—	22.7(2)	27.50(5)	
		(2,0,1)	37.21(5)	—	27.26(9)	21.63(4)	
		pM		26.3	24.9	19.0	10.7
	 IDAPr(3,4-HP) ₂ ^b		(2,-2,2)	44.00	—	32.05	—
		(1,-1,1)	—	18.23	—	—	
		(2,3,3)	89.53	84.97	76.64	—	
		(2,2,3)	85.54	80.16	71.72	—	
		(2,1,3)	79.90	74.64	66.21	—	
		(2,0,3)	74.26	68.44	60.18	—	
		(1,3,1)	33.59	33.21	30.44	27.28	
		(1,2,1)	—	—	27.71	—	
		(1,1,1)	31.16	28.83	25.37	18.93	
		(1,0,1)	26.16	24.30	20.35	13.30	
	pM		25.8	22.9	18.8	9.7	
 3,4-DMHP ^c		(1,0,1)	15.10	13.17	12.20	7.19	
		(1,0,2)	26.61	25.43	23.25	13.53	
		(1,0,3)	35.88	35.76	32.62	—	
		pM		19.3	19.4	16.1	16.1
 EDDA		(1,-2,1)	3.50(3)	9.33(5)	—	—	
		(1,-1,1)	—	14.14(2)	—	—	
		(1,0,1)	14.99(1)	16.43(4)	10.70(2)	11.1	
		pM		17.1	22.9	13.1	9.8
DTPA ^d		pM	24.6	20.9	15.2	14.8	
DOTA ^d		pM	24.3	18.8	13.2	17.9	
Desferrioxamine (DFB) ^{e,f}		pM	26.5	22.4	19.3	6.6	
Transferrin		pM	20.3 ^g	20.3 ^h	14.5 ⁱ	—	

^a pM = $-\log[M]$ with $C_L/C_M = 10$ and $C_M = 10^{-6}$ M; (p,q,r) means a metal complex species with stoichiometry $M_pH_qL_r$. ^b Ref. 14. ^c Ref. 18. ^d Ref. 19. ^e Ref. 20. ^f Ref. 21. ^g Ref. 22. ^h Ref. 23. ⁱ Ref. 24.

Al-overloaded mice. To evaluate the specificity of this compound for chelating to these hard metal ions, but sparing the biologically relevant zinc, complexation studies with zinc have also been carried out. The metal chelation strength and the coordination modes have been evaluated by potentiometric and spectroscopic methods (UV-Vis and NMR). Some molecular modeling DFT calculations also gave support to the coordination modes. Results of *in vivo* assays are presented in the assessment of the metal sequestering efficiency (clearing efficacy) of this chelating agent when administered to an animal model (mice) preloaded with the radiotracer ⁶⁷Ga-citrate. The results of the solution and

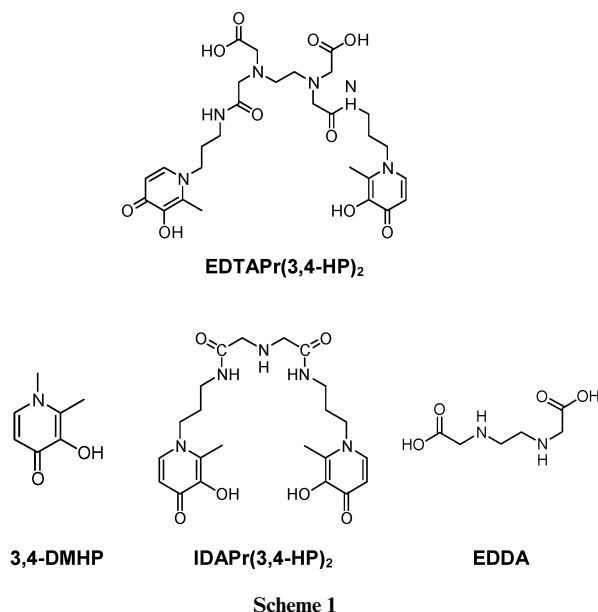
in vivo studies are compared with those obtained with other 3,4-HP analogues, including the currently used iron-chelating drug (DFP).

2. Results and discussion

Protonation of the ligands

To study the metal complexation with EDTAPr(3,4-HP)₂, we have used the protonation constants previously reported for this ligand,¹⁷ as depicted in Table 1, which also contains the

corresponding values for some model compounds (EDTAPr(3,4-HP)₂,¹⁴ 3,4-DMHP,¹⁸ and EDTA,¹⁹ see Scheme 1).



Metal complexation

Metal complexation with a model ligand EDTA. The molecular structure of the ligand EDTAPr(3,4-HP)₂ is based on two hydroxypyridinone moieties connected to a polyaminocarboxylic scaffold, the ethylenediaminetetraacetic acid (EDTA). Besides the hydroxypyridinone chelating arms, there are still two free ethylenediamine carboxylates, hereafter named as the EDTA segment. Since EDTA is also a good chelating agent, we decided to start the metal complexation studies with the characterization of the EDTA–M(III) systems, using our experimental conditions ($I = 0.2$ KCl, $T = 25$ °C). An analysis of the potentiometric titration curves obtained for the different EDTA–M(III) systems ($M = \text{Fe}, \text{Al}, \text{Ga}$), at 1 : 1 ligand-to-metal ion ratio (Fig. S1†), show that for the Al system the precipitation started at quite an early stage (*ca.* pH 3) due to hydrolysis, thus indicating that EDTA has a low affinity for Al(III) (and that the Al(III) coordination by EDTAPr(3,4-HP)₂ should involve mostly the hydroxypyridinone groups). In the case of Fe(III) and Ga(III) complexation with EDTA, at 1 : 1 molar ratio, the precipitation occurs at *ca.* pH 5. Fitting of all the experimental data registered before the precipitation of the Fe(III)- and Ga(III)-containing systems resulted in equilibrium models with the absence of any dinuclear complexes and formation of only mononuclear species, ML, followed by mixed hydroxo species, namely MOHL and M(OH)₂L in both systems. To our surprise, comparison between the corresponding titration curves obtained for the Fe(III) and the Ga(III) systems always indicated a slightly higher drop in pH on the Ga(III) titration curve than on the corresponding Fe(III) curve, thus suggesting a higher stability for the gallium complexes. The calculated cumulative formation constants (Table 1) reflect those curve-profile differences, which are also in agreement with the literature values ($\log\beta_{\text{FeL}} = 15.50$,²⁵ $\log\beta_{\text{GaL}} = 18.15$,²⁶ $L = \text{EDTA}$).

Iron complexation with EDTAPr(3,4-HP)₂. The complexation behaviour of EDTAPr(3,4-HP)₂ towards the M³⁺ hard metal ions ($M = \text{Fe}, \text{Al}, \text{Ga}$) in aqueous solutions, was studied by potentiometric and spectrophotometric techniques at various ligand-to-metal ion molar ratios. Representative potentiometric titration curves are shown in Fig. 1, for the ligand alone and in the presence of Fe³⁺, at 1 : 0.43 to 1 : 1.6 ligand-to-metal ion molar ratios. Analysis of the titration curves for the binary systems shows: (i) the existence of a considerable drop in pH at the beginning of the titration, as compared with that of the ligand, thus indicating high affinity of the ligand for this metal ion and measurable complexation below pH 2; (ii) if a significant amount of excess ligand is present ($L : M = 1 : 0.43$), the deprotonation of the ammonium group (pH range *ca.* 6–8) does not seem greatly affected by the presence of the metal ion, thus suggesting that under these conditions only the hydroxypyridinone (HP) moieties are coordinated to the metal ion, while the “EDTA” part of the ligand molecule is not involved in the coordination. However, for a 1 : 1 stoichiometry, there is a change in the titration curves corresponding to the ammonium deprotonation. Therefore, under these conditions, the eventual interaction between the “EDTA” part of the ligand and the metal ion could be hypothesized because the two HP moieties are not enough to complete the coordination sphere of Fe(III). If metal excess is present, hydrolytic processes can also occur.

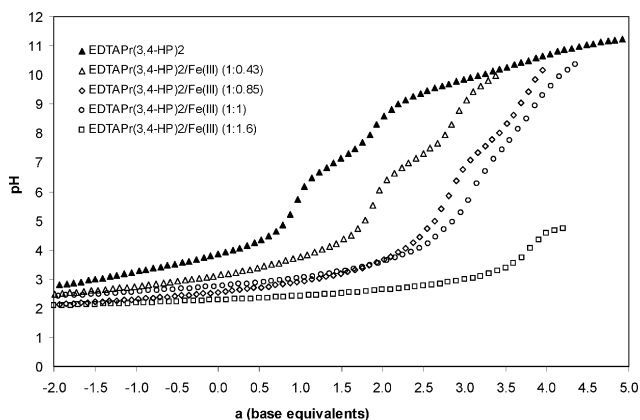


Fig. 1 Potentiometric titration curves of aqueous solutions containing EDTAPr(3,4-HP)₂, $C_L = 2.63 \times 10^{-3}$ M, alone (\blacktriangle), and in the presence of Fe³⁺ at: 1 : 0.43 (\triangle) and 1 : 0.85 (\diamond) ligand-to-metal molar ratios, $C_L = 3.50 \times 10^{-3}$ M; 1 : 1 (\circ) and 1 : 1.6 (\square) ligand-to-metal molar ratios, $C_L = 1.98 \times 10^{-3}$ M. $I = 0.2$ M KCl, $T = 25.0$ °C.

Since the coordination of the ligand to Fe(III) starts at pH below 2, the cumulative formation constants of the complex species formed at such a low pH were determined by spectrophotometry as previously reported for other bis-hydroxypyridinone ligands.^{14,16,27,28} Besides the spectrophotometric titration at very low pH, some other titrations in the whole measurable pH range were made using different ligand-to-metal ion ratio and some of them are presented in Fig. 2.

Analysis of the spectra obtained at pH < 2 provided evidence that the metal coordination starts at very low pH (pH < 0.8) (Fig. S2†) with formation of a mono-chelated species ($\lambda_{\text{max}} = 565$ nm); at pH 2, the spectra presents a band ($\lambda_{\text{max}} = 510$ nm) which can be attributed to the bis-chelated species.^{14,29,30} Since this

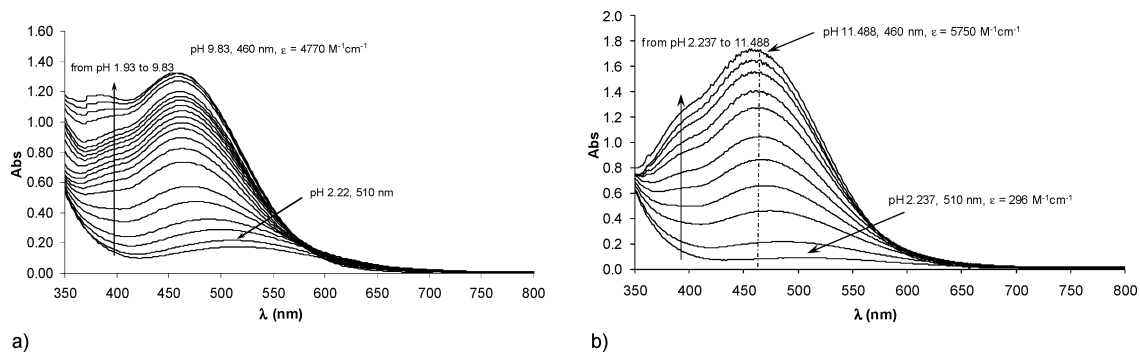


Fig. 2 Absorption spectra registered at different pH values for the EDTAPr(3,4-HP)₂-Fe(III) system at: (a) 1 : 1 ligand-to-metal molar ratio, $C_L = C_{Fe} = 2.78 \times 10^{-4}$ M, and (b) 2 : 1, with $C_L = 6.21 \times 10^{-4}$ M. $I = 0.2$ M KCl, $T = 25.0$ °C.

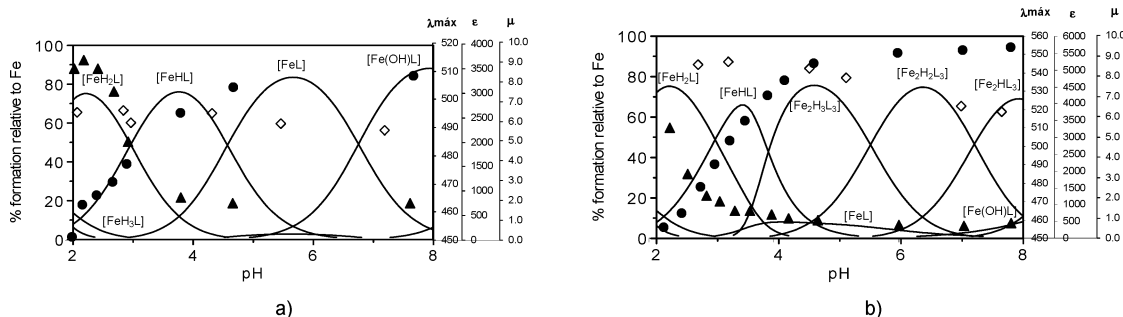


Fig. 3 Concentration distribution curves of the Fe-containing species for the system EDTAPr(3,4-HP)₂-Fe(III) at: (a) 1 : 1 ligand-to-metal molar ratio ($C_L = C_{Fe} = 1.65 \times 10^{-4}$ M); and (b) 2 : 1 ligand-to-metal molar ratio ($C_L = 6.21 \times 10^{-4}$ M, $C_{Fe} = 3.01 \times 10^{-4}$ M). pH dependence of λ_{max} (▲), molar absorptivity (\bullet), of UV-Vis spectra, and molar magnetic moment (μ) of [Fe(III)-EDTAPr(3,4-HP)₂] complexes. $I = 0.2$ M KCl, $T = 25.0$ °C.

is a charge transfer (CT) band between the hydroxypyridinone oxygen atoms and Fe^{3+} , and no spectral changes are expected from the deprotonation of the amine nitrogen of the “EDDA” part of the molecule, it is not possible to infer about the involvement of the “EDDA” moiety in the metal coordination. Above pH 2, both the stoichiometric systems presented blue-shifts of the CT absorption bands, thus indicating the formation of species with increased number of coordinating units around the metal ion. Spectral bands with $\lambda_{\text{max}} = 460$ nm are characteristic of tris-chelated species (three hydroxypyridinone units coordinated to the Fe^{3+} metal ion).^{14,30,31} However, there is no possibility to saturate all of the six coordination sites by one ligand *via* hydroxypyridinonate type chelates. Therefore, under these ligand-to-metal stoichiometric conditions (2 : 1), it can be assumed that one ligand molecule can bridge two bis-chelated iron centers to complete their coordination sphere, which should correspond to the formation of dinuclear species $\text{Fe}_2\text{H}_x\text{L}_3$ ($x = 0,1,2,3$). On the other hand, mixed hydroxypyridinone–ligand–hydroxo species (with μ_2 -hydroxo bridged bonds) have also been reported with a similar λ_{max} value.¹⁴ Under the experimental spectrophotometric conditions, the occurrence of precipitation was not observed. The fitting analysis of the experimental spectra with equilibrium models (PSEQUAD program)³¹ allowed the calculation of cumulative formation constants presented in Table 1; the agreement between simulated and experimental spectra of some complex species (Fig. S2†) also gave support to the assumed equilibrium models. The calculated cumulative formation constants allowed the calculation of the concentration distribution species with pH depicted in Fig. 3. This figure also shows the dependence of

the λ_{max} and of the molar absorptivity on the pH, where values are according to the expected ones for the corresponding model complex species. The variation of the magnetic moment along the same range of pH measured under the same conditions used for the complexation studies, is also included therein, which is aimed at elucidating the presence of dinuclear iron(III) complexes.

At $T = 298$ K, for the 1:1 stoichiometry (Fig. 3(a)), the measured magnetic moments μ_M (*ca.* 6 MB) are in agreement with reported values for non-interacting mono-ferric complexes in the solid state (5.9 MB).³² On the other hand there is no appreciable decrease in the value along the studied pH range indicating the absence of dinuclear species with strong anti-ferromagnetic interactions between the two Fe(III) sites, namely binuclear species with bridging hydroxo groups, μ_2 -oxo species ($\mu_M = 3.4$ MB, at 300 K).³³ Also for the 1:2 stoichiometric conditions (Fig. 3(b)), up to pH 7, there is no variation in μ_M , indicating that the dinuclear species should have the ferric centres separated enough to prevent any strong anti-ferromagnetic interactions. Above that pH, some decreasing is observed in μ_M , which can be due either to the formation of some bridging hydroxo groups or, most probably, just to some undetected minor precipitation of hydroxo–ligand mixed complex species.

Aluminium(III) complexation with EDTAPr(3,4-HP)₂. To study the EDTAPr(3,4-HP)₂-Al(III) system, potentiometric titrations were carried out at 2:1 and 1:1 ligand-to-metal ion ratios (Fig. 4). Analysis of the potentiometric curve for the 1:1 stoichiometric conditions indicates that the complex formation starts at pH *ca.* 2, most probably with formation of a

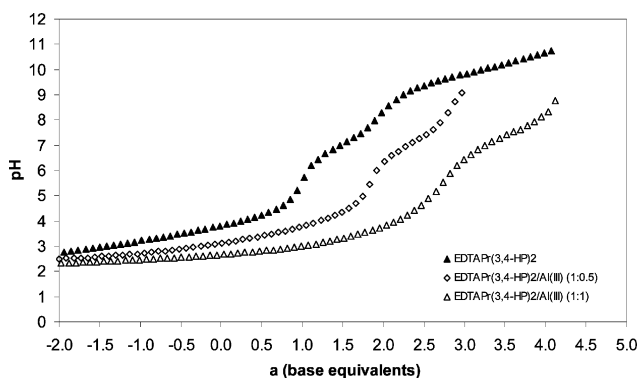


Fig. 4 Potentiometric titration curves of aqueous solutions containing EDTAPr(3,4-HP)₂, $C_L = 2.63 \times 10^{-3}$ M, alone (▲), and in the presence of Al³⁺, at the ligand-to-metal molar ratios: 1:0.5 (◇) and 1:1 (△); $C_L = 3.50 \times 10^{-3}$ M. $I = 0.2$ M KCl, $T = 25.0$ °C.

mono-chelated species, AlH₄L, containing only one hydroxypyridinone group coordinated to the metal ion, with eventual coadjuvation of one carboxylic group.

Stepwise release of one proton from the EDDA backbone and two protons from the second hydroxypyridinone moiety leads to the formation of the bis-chelated species (AIL). The fact that the release of the fourth proton from the complexes seems to occur at a lower pH (*ca.* 4) than for the ammonium proton of the free ligand ($pK = 7.04$) could be due to either the interaction of the carboxylate with the metal ion (so the ammonium proton could be pushed by the metal ion) or, most probably, to some hydrolytic process (so the species formed could actually be Al(OH)LH instead of AIL). For the 1:2 stoichiometry, tris-chelated species are expected to be formed as 2:3 dimeric species, Al₂H_xL₃, ($x = 0, 1, 2, 3$). The formation of the bis-chelated complex with Al(III) starts at *ca.* pH = 2 with subsequent stepwise deprotonation with increasing pH. Fitting analysis of the titration curve leads to an equilibrium model involving mononuclear and binuclear species (see Table 1) in different ratios, depending on the stoichiometric conditions. The $\log\beta$ values calculated for the different complex species with this tetradentate ligand are consistent with the corresponding values for the bidentate analogue (3,4-DMHP) (Table 1). Representative examples of concentration distribution curves for the Al(III) containing system are shown in Fig. 5.

Aimed at gaining some support for the assumed equilibrium models, ¹H NMR spectra were also registered for the ligand EDTAPr(3,4-HP)₂ alone, and in the presence of Al(III) at 1:1 and

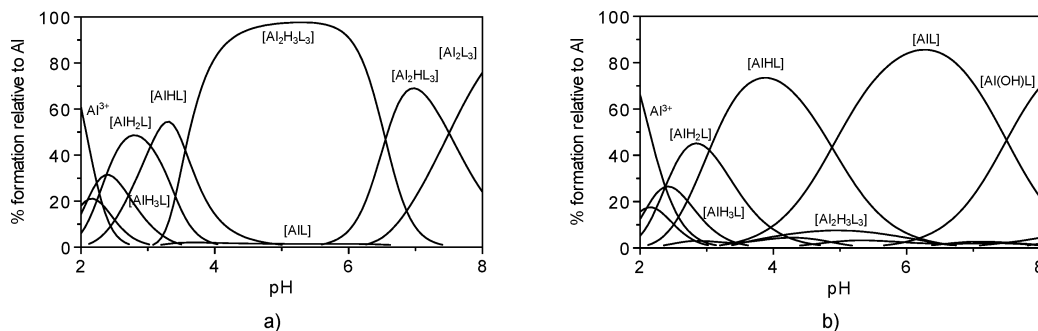


Fig. 5 Concentration distribution curves of the Al-containing species for the system EDTAPr(3,4-HP)₂-Al(III) at ligand-to-metal molar ratios: (a) 1:1 and (b) 2:1; $C_L = 3.5 \times 10^{-3}$ M. $I = 0.2$ M KCl, $T = 25.0$ °C.

1:3 (M:L) stoichiometry, at different pH values. Comparison of the spectra registered for the ligand and for the complex systems at both ratios, showed a clear change in chemical shifts of the peaks corresponding to the hydroxypyridinone, but no change in the proton peaks of the “EDDA” part of the ligand molecule (Fig. S3†). These results are especially relevant for the 1:1 stoichiometry, indicating that the ligand-to-Al(III) coordination does not involve the EDDA arm, but only the hydroxypyridinone moieties. The titration stopped at *ca.* pH 4 due to precipitation, which can be a result of the formation of the hydrolytic species (eventually Al(OH)LH instead of AIL) and so the hydrolysis might start before the deprotonation of the ammonium proton. The changes induced on the aromatic hydroxypyridinone protons by the Al-complexation are clearly shown in Fig. 6, providing evidence for the involvement of the pyridinone arms in the metal ion coordination. Deconvolution of the ¹H NMR spectra for the Al-ligand system at different pH values by the *Mestre C* program³⁴ allowed a comparative analysis of the relative intensities

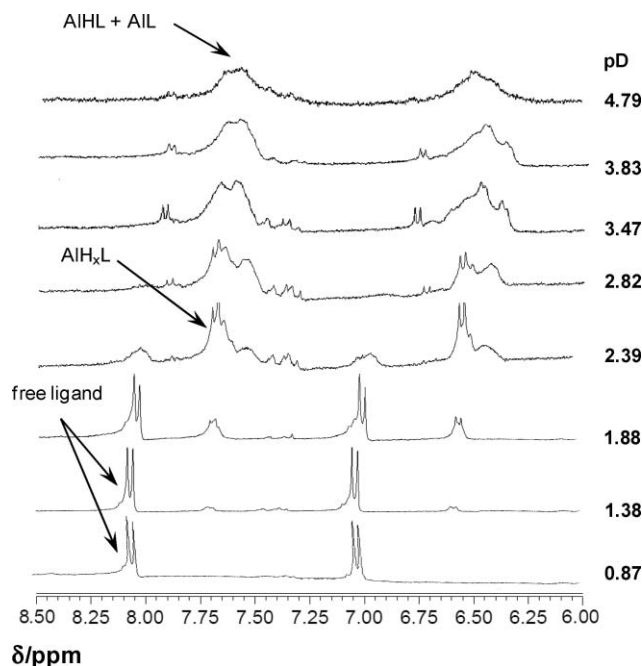


Fig. 6 ¹H NMR spectra at indicated pD corresponding to the hydroxypyridinone ring protons of solutions containing EDTAPr(3,4-HP)₂ and Al³⁺ at 1:1 ligand-to-metal molar ratio, $C_L = 2.0 \times 10^{-2}$ M.

Table 2 Calculated relative percentage of the ^1H NMR peaks specified. The values in parenthesis represent the species percentage given by the potentiometric result for the same conditions ($C_L = C_{Al} = 2 \times 10^{-2}$ M)

Peaks	pD = 0.87	pD = 1.38	pD = 2.39	pD = 2.82	pD = 3.47	pD = 4.79	Attributions
A	100 (100)	83 (92)	24 (12)	3 (2)	—	—	Free hydroxypyridinone
B	—	17 (8)	52 (48)	67 (68)	37 (33)	—	AlH_xL ($x = 2, 3, 4$)
C	—	—	24 (33)	30 (30)	53 (67)	100 (100)	AlH_xL ($x = 0, 1$)

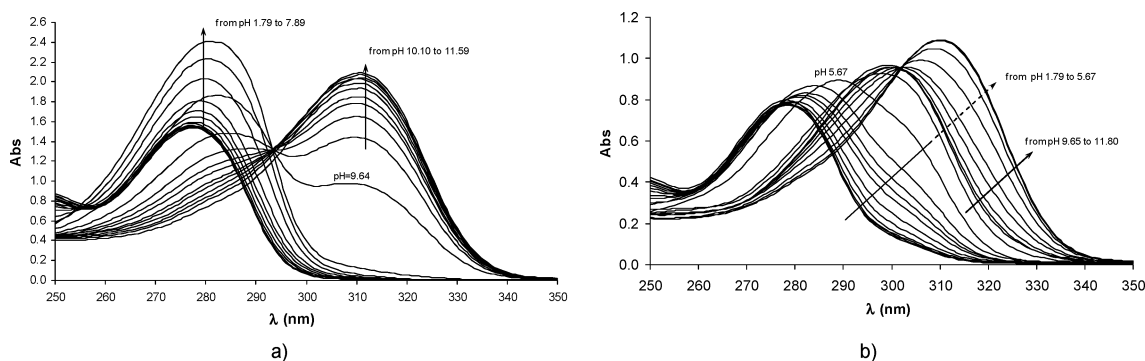


Fig. 7 Absorption spectra registered at different pH values for (a) the ligand $\text{EDTAPr}(3,4\text{-HP})_2$ alone, $C_L = 1.0 \times 10^{-4}$ M; (b) for the $\text{EDTAPr}(3,4\text{-HP})_2\text{-Ga(III)}$ system, $C_L = 5.25 \times 10^{-5}$ M, $C_{Ga} = 2.01 \times 10^{-5}$ M. $I = 0.2$ M (KCl, HCl), $T = 25.0$ °C.

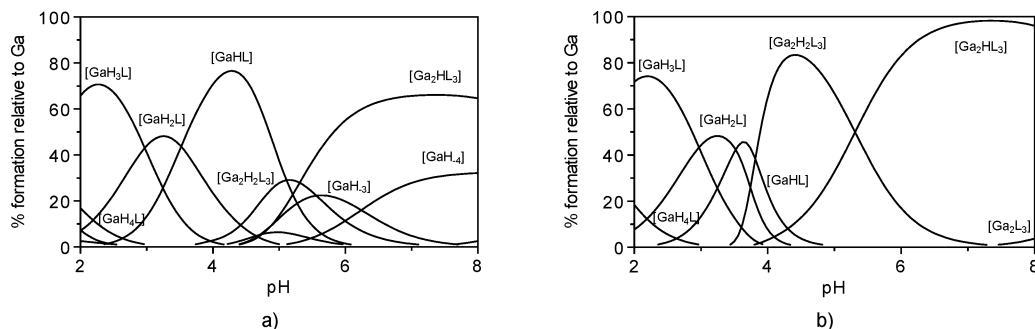


Fig. 8 Concentration distribution curves of the Ga-containing species for the system $\text{EDTAPr}(3,4\text{-HP})_2\text{-Ga(III)}$ at the ligand-to-metal molar ratios: (a) 1 : 1 and (b) 2 : 1; $C_L = 5.25 \times 10^{-5}$ M. $I = 0.2$ M KCl, $T = 25.0$ °C.

of the individual peaks with the species distribution curves and enabled a rough peak attribution to the species in solution. Table 2 includes the calculated relative percentages for each peak, and their assignment to the corresponding species. We can conclude that there is a reasonably good fit between the values obtained for the concentration distribution species on the basis of the ^1H NMR spectroscopic signals and the potentiometric results.

Ga(III) complexation with $\text{EDTAPr}(3,4\text{-HP})_2$. For this complexation study, only spectrophotometry was used instead of pH-potentiometry because the higher concentration conditions demanded for this technique led to precipitation. Although no characteristic bands belong to the Ga(III) complexes, comparison between the spectra obtained for the ligand alone and in the presence of the metal ion (Fig. 7), suggests considerable changes due to the formation of a complex species with high stability.

Fitting analysis of the spectra obtained at different pH values and various ligand-to-metal ion stoichiometric conditions was

performed with the PSEQUAD program,³¹ which input file includes the calculated molar absorptivity as fixed data. Since this spectra analysis involves only data from the ligand itself, the corresponding mathematical fitting was more difficult than for the other complex systems; however, it was possible to find a self-consistent equilibrium model, where the complex species and stability constants are presented in Table 1 and the corresponding concentration distribution curves are depicted in Fig. 8.

Molecular modeling studies. In order to obtain some structural information on the aluminium complex, a molecular modeling study was performed based on molecular mechanics, AM1 semi-empirical, and DFT calculations. These methods were systematically employed³⁵ for this type of molecular systems.

To obtain the final structure, we applied a general procedure presented in the specialized literature.^{36–38} Briefly, the starting structures generated by the CACHE editor³⁹ were firstly optimized by the MM3 method. The most stable conformer obtained for

every case was successively optimized by AM1 (vacuum) and AM1 (COSMO) methods. Finally, for the most stable conformer found by this last method, its geometric optimization was carried out using the Density Functional Theory and the B3LYP hybrid functional, in the Gaussian03 program.⁴⁰

Due to the complexity of the computed structures, DFT calculations were performed in two steps: firstly, a structure was obtained using the STO-3G basis set and its geometry optimization was further refined during the second step, using a more accurate basis set, namely 6-31G**. No symmetry constraints were enforced during geometry optimization. Both methods indicate the same type of structure for the most stable AlL complex, and Fig. 9 presents the most stable conformer obtained by the DFT calculations.

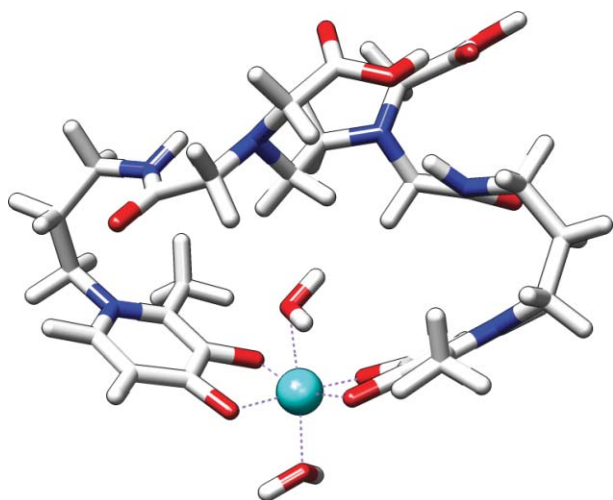


Fig. 9 The most stable conformer of the aluminium complexes obtained by the DFT calculations.

The only difference is in the numerical value of the energy (-2533.0398418 Hartree using STO-3G and -2566.0642645 Hartree using 6-31G**). It can be seen from the structure that the coordination of the aluminium atom involves two hydroxypyridinone arms ($2 \times \{O, O\}$). The other two extra-coordinating sites are satisfied by two water molecules. No other part of the EDTA moiety is involved in the complexation of aluminium. An interesting aspect is that even without symmetry constraints imposed, the aluminium atom adopts an octahedral configuration. The computed structure shows a very good agreement with the

theory and it is extremely well correlated with the experimental NMR data that we obtained.

Chelating selectivity of the EDTAPr(3,4-HP)₂. As a potential Fe(III)- and Al(III)-chelating agent, EDTAPr(3,4-HP)₂ should present a high affinity and specificity for these M(III) to allow for their decorporation without depletion of other bioavailable essential metal ions such as Zn(II). Therefore, EDTAPr(3,4-HP)₂-Zn(II) complexation studies were also performed by potentiometric titrations at different stoichiometric conditions. From the potentiometric titration curves (Fig. S4†), it was not clear whether there was any involvement of the “EDDA” part of the molecule in the coordination of the Zn(II) metal ion. There was some change in the shape of the titration curves but for pH values at which the hydrolysis may also occur. The fitting of those titration curves leads to stability constant values (Table 1) and the species distribution curves (Fig. 10).

In order to gain a better understanding of the coordination modes involved in this equilibrium system, some ¹H NMR studies were made. The ¹H NMR titration curves of the ligand in a D₂O solution was compared with two sets of ¹H NMR titration curves of the EDTAPr(3,4-HP)₂-Zn(II) system at 1 : 1 and 1 : 2 ligand-to-metal ion molar ratios. A comparative analysis of both sets of spectra (see spectra for selected pD in Fig. S5†) show that there are interactions with both parts of the molecule (the “EDDA” part and the hydroxypyridinone moieties), as indicated by the changes in the NMR peaks corresponding to these two molecular segments.

A detailed analysis of those spectra shows that at low pH (pD *ca.* 0.6–0.7) there is no appreciable modification of the ligand spectra in the presence of the metal ion. At pD = 1.5–1.7, some changes in the peaks corresponding to the EDDA skeleton are noticeable, increasing with pH. At higher pH (pD *ca.* 3.7–4.6), a number of changes were observed in the aromatic region of the spectra, indicative of the participation of the hydroxypyridinone groups in the zinc coordination, although there are still some changes in the spectra with regards to the “EDDA” skeleton, which indicate interactions of that molecular segment with the metal ion.

From all those observations, we can say that the zinc coordination starts with the “EDDA” skeleton of the ligand molecule but finishes with a bis-hydroxypyridinone coordination mode. In fact, the $\log \beta$ value (37.19) obtained for the first complex species (ZnH_4L) is in agreement with a EDDA-Zn(II) coordination contribution (*ca.* 11) plus the pK_a values of the four hydroxypyridinones protons. The subsequent deprotonation processes

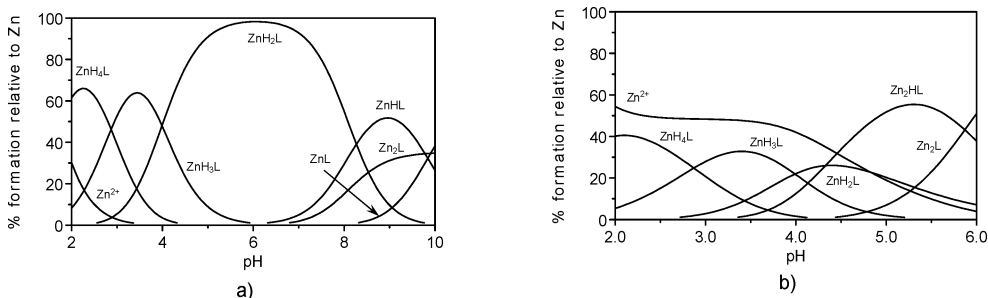


Fig. 10 Concentration distribution curves of the Zn-containing species for the system EDTAPr(3,4-HP)₂-Zn(II) at the ligand-to-metal molar ratios: (a) 1 : 1 and (b) 1 : 2; $C_L = 3.0 \times 10^{-3}$ M. $I = 0.2$ M KCl, $T = 25.0$ °C.

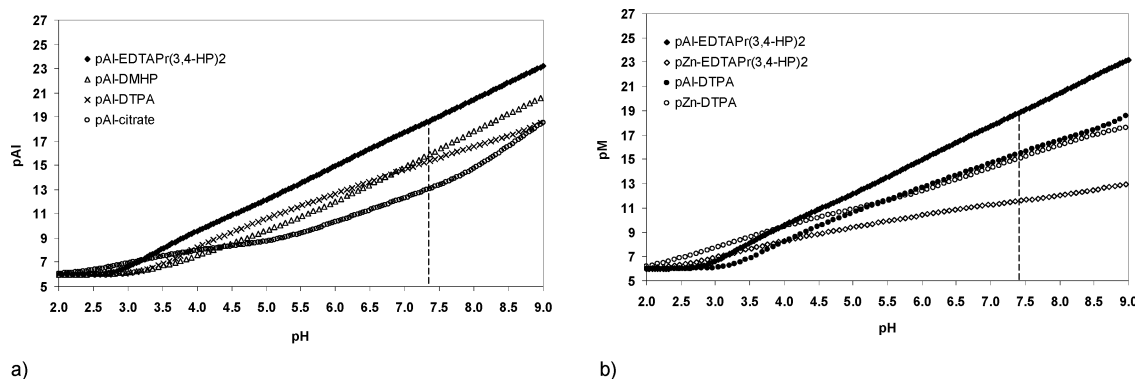


Fig. 11 pM ($M = \text{Al}, \text{Zn}$) versus pH for the systems: $\text{Al(III)-EDTAPr(3,4-HP)}_2$, Al(III)-3,4-DMHP , Al(III)-DTPA , Al(III)-citrate and $\text{Zn(II)-EDTAPr(3,4-HP)}_2$ and Zn(II)-DTPA ; $\text{pM} = -\log[M]$ with $C_L/C_M = 10$ and $C_L = 1 \times 10^{-5} \text{ M}$.

are according to the stepwise release of two pyridinium protons, affording ZnH_3L and ZnH_2L ; the final hydroxypyridinone deprotonation/coordination starts at *ca.* $\text{pH} = 6$, leading to the formation of hydroxypyridinone bis-chelated species. Such a behaviour can be rationalized by the fact that the aminoacid is the less basic group and so zinc can compete with the corresponding protons in acidic conditions whereas, at neutral pH conditions, the hydroxypyridinone chelates are much more stable than those with the EDDA moiety.

Comparative analysis of the complexation ability

A comparison between the metal (M) chelating affinities of the ligands with different proton dependency and denticity can be made on the basis of pM values ($\text{pM} = -\log[M]$) with $C_L/C_M = 10$ and $C_M = 10^{-6} \text{ M}$ at a specific pH, usually the physiological pH (7.4). Therefore, pM values were calculated for the metal systems with the ligand in study as well as for a set of common synthetic and biological ligands (see Table 1). It is clearly shown that under micromolar conditions that prevail in biological systems, EDTAPr(3,4-HP)_2 presents a much higher metal chelating efficacy than the mono-hydroxypyridinone derivative, 3,4-DMHP (deferiprone) ($\Delta\text{pFe} = 7$). Thus, it can be predicted to be a better scavenger for these type of hard metal ions than deferiprone. It also presents a slightly higher chelating ability than the bis-hydroxypyridinone analogue, IDAPr(3,4-HP)_2 ,¹⁴ which may be due to the higher flexibility of the present ligand. Additionally, EDTAPr(3,4-HP)_2 shows a much higher chelating efficacy and specificity for these M^{3+} metal ions than some of the polyaminocarboxylate ligands (DTPA and DOTA)¹⁹ with clinical applications in imaging with ^{68}Ga . The present ligand shows a chelating strength similar to that of DFO for this set of metal ions,^{20,21} while from complexation data with transferrin (Table 1) it seems likely that EDTAPr(3,4-HP)_2 can compete with apotransferrin for this set of metal ions.²²⁻²⁴ However, since the mono-hydroxypyridinone deferiprone proved to be able to mobilize iron from several iron-containing proteins such as ferritin and transferrin,⁴¹ an identical role can be postulated for the present di-hydroxypyridinone, eventually with even higher efficacy.

Concerning the Zn-affinity, the polyaminocarboxylate ligands with clinical applications (DOTA and DTPA)¹⁹ present the highest values, followed by the aminocarboxylic-hydroxypyridone ligand, EDTAPr(3,4-HP)_2 , as expected. Although the difference between

the Al- and Zn-chelating affinities of the present ligand ($\Delta\text{pM} = 8.2$) is lower than that found for 3,4-DMHP ($\Delta\text{pM} = 9.9$), the difference is still high enough to conclude that the EDTAPr(3,4-HP)_2 ligand is a strong and selective Al-chelating agent under physiological pH conditions. In the case of Fe(III) , this selectivity is even better with the bis-chelated ligand, with $\Delta\text{pM} = 15.7$ instead of the 13.1 of 3,4-DMHP. A further comparison between the Al-chelating affinities of several ligands and the Al/Zn chelating selectivity, along a wide pH range (2–9), is also graphically illustrated in Fig. 11(a) and 11(b), respectively. Fig. 11(a) shows that the new chelating agent presents the highest Al-affinity along a wide pH range (3.5–9), in opposition to deferiprone (3,4-DMHP) which, for acidic-neutral pH conditions, is overcome by the aminocarboxylic ligand (DTPA). Fig. 11(b) confirms the high Al/Zn selectivity of the new chelating agent in a wide range of pH, excluding the acidic ($\text{pH} < 4$).

Biodistribution studies. The results on the whole body ^{67}Ga excretion data for the complexes are presented in Fig. 12 as a percentage of the injected dose, illustrating the main differences between the ^{67}Ga –(3-hydroxy-4-pyridinone) complexes and that of ^{67}Ga –citrate.

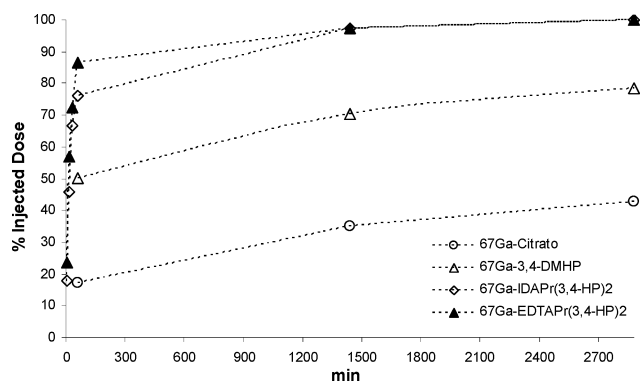


Fig. 12 Whole body excretion expressed as a percentage of injected dose (% I.D.) of ^{67}Ga –citrate, ^{67}Ga –3,4-DMHP, ^{67}Ga – IDAPr(3,4-HP)_2 , and ^{67}Ga – EDTAPr(3,4-HP)_2 complexes, 5, 15, 30, 60, 1440 and 2880 min after intravenous administration of the radiotracer in female mice ($n = 3-5$).

The administration of a ^{67}Ga – EDTAPr(3,4-HP)_2 complex solution interferes with the normal biological distribution profile of the tracer leading to a highly increased excretion rate of radioactivity

from the whole animal body, as compared with the excretion of the ^{67}Ga -citrate form, similarly to the results obtained with other bis-(3-hydroxy-4-pyridinone) ligands, $\text{IDAPr}(3,4\text{-HP})_2$.¹⁴ Thus, the enhancement of the ^{67}Ga excretion rate is probably due to the higher metal-binding affinity of these aminoacid-bis(hydroxypyridinone) ligands, as compared to that of citrate and the mono-hydroxypyridinone, 3,4-DMHP. (More details about the biodistribution profile are published in ref. 17).

3. Experimental

Materials and methods

All the reagents used were analytical-grade commercial reagents. The ligand, $\text{EDTAPr}(3,4\text{-HP})_2$, was synthesized according to standard synthetic methodologies,¹⁷ although in the present synthesis the purification of the compound also involved a chromatographic separation with Shephadex (LH20) using water (pH = 7) as eluent.

Potentiometric and spectrophotometric studies

Reagents and solutions. Aqueous stock solutions of M(III) (M = Fe, Ga, Al) were prepared from the corresponding chloride salts. ZnO (Reanal) was dissolved in a known amount of HCl solution (0.1 M). The exact concentration of the metal ion was calculated gravimetrically *via* precipitation of the quinolin-8-olate and the containing acid was determined by potentiometric titration. The titrant was non-carbonated 0.2 M KOH solution, which was standardized with a 0.025 M potassium hydrogen phthalate solution, using the Gran's method.⁴²

Potentiometric measurements. The potentiometric measurements were performed with a MOLSPIN pH-Meter, equipped with a Metrohm 6.0234.100 combined electrode and a Mol-AcS microburette controlled by a computer at 25.0 °C and ionic strength $I = 0.2\text{ M}$ (KCl). To calibrate the electrode, the method described by Irving *et al.* was used⁴³ which meant that the pH-metric reading could be converted into hydrogen ion concentration. The water ionization constant, K_w , was found to be $10^{-13.76}$ under the conditions employed. All the samples were CO_2 -free by passing argon on the top of the sample in the potentiometric cell. The pH-metric titrations were performed throughout the pH range ≈ 2.0 –11.0. All titrations started at pH ~ 2 after the addition of the necessary amount of acid. Samples of 3.0 mL were used. The ligand concentrations were varied in the range 1.00 – $3.50 \times 10^{-3}\text{ M}$. Different ligand-to-metal ion molar ratios were used (2 : 1, 1 : 1, 1 : 2).

Spectrophotometric measurements. A HP 8453 spectrophotometer was used to record the spectra in the region 250–800 nm. The ligand concentrations were varied in the range 10^{-5} – 10^{-3} M . Different ligand-to-metal ion ratios were used (2 : 1, 1 : 1, 1 : 2). The pH values were measured using a MOLSPIN pH-Meter equipped with a Metrohm 6.0234.100 combined electrode.

Calculations. The proposed equilibrium models were based on the chemical structure of the ligand and the calculations of the overall stability constants, $\beta_{M_p H_q L_r} = [\text{M}_p \text{H}_q \text{L}_r] / [\text{M}]^p [\text{H}]^q [\text{L}]^r$. They were obtained by fitting analysis of the titration data with the PSEQUAD computer program³¹ and using the literature data for the hydrolytic species.^{44,45} The selection of the equilibrium

models was based on the critical analysis of the weighted residuals, the statistical parameters (χ^2 , σ)⁴⁶ and graphical comparisons between the experimental and simulated potentiometric curves. For very acidic conditions (pH < 2), the stability constants of the corresponding Fe(III) and Ga(III) complexes were calculated from the spectrophotometric data using the PSEQUAD program.³² The results were accepted for the fitting parameter smaller than 2×10^{-2} . The HYSS program⁴⁷ was used to get the concentration distribution curves.

^1H NMR measurements

^1H NMR titrations were performed in a Varian Unity 300 spectrometer at probe temperature. The samples were prepared in D_2O and the pD was measured with a Thermo Orion 420A pH meter and a Mettler Toledo (U402-M3-S7/200) micro-electrode. Since the electrode was calibrated with standard buffer aqueous solutions, pH* is the direct value measured by the pH meter and the final pD was calculated as $\text{pD} = \text{pH}^* + 0.4$.⁴⁸ The pH* change was performed with DCl and KOD solutions diluted in D_2O . Chemical shifts (δ ppm) were measured using sodium 3-(trimethylsilyl)-[2,2,3,3- D_4]propionate (DSS) as an internal reference ($\delta = 0$ ppm). The iron(III) molar magnetic susceptibilities (χ_M) were measured in D_2O solution as a function of pD by the Evans method,⁴⁹ and the corresponding magnetic moments were calculated ($\mu_M = 2.84(\chi_M T)^{1/2}$),⁵⁰ for both the Fe(III):L stoichiometries under the same experimental concentration conditions used for the potentiometric measurements, and $T = 298\text{ K}$.

4. Conclusions

The complex formation of an aminocarboxylic-bis-hydroxypyridinonate ligand, $\text{EDTAPr}(3,4\text{-HP})_2$, was studied in aqueous solution, and the results demonstrate that in a wide pH range, and diluted conditions prevailing *in vivo*, this new compound has a higher efficacy for chelating hard metal ions (*e.g.* Fe^{3+} , Ga^{3+} , Al^{3+}) than the mono-hydroxypyridinone, deferiprone (a drug clinically used), and also some bioligands (*e.g.* citric acid and transferrin). The excellent solution properties of this compound, namely the balanced hydrophilicity, high complexation ability towards iron and aluminium, and its good Fe/Zn and Al/Zn selectivity, together with the *in vivo* behaviour, namely the favourable biodistribution pattern of this new chelating agent with rapid clearance of ^{67}Ga -overload mice from main organs and the high rate of metal excretion, suggest its potential usefulness as an *in vivo* Al- and Fe-decorporating agent, without zinc depletion.

Acknowledgements

The authors thank the Portuguese Fundação para a Ciência e Tecnologia (FCT) (Project PDCT/QUI/56985/2004), the Hungarian Scientific Research Fund (OTKA T049612) and the Portuguese–Hungarian bilateral program.

References

- 1 G. Crisponi and M. Remelli, *Coord. Chem. Rev.*, 2008, **252**, 1225–1240.
- 2 M. A. Santos, *Coord. Chem. Rev.*, 2002, **228**, 187–203.
- 3 N. F. Olivieri, *N. Engl. J. Med.*, 1999, **341**, 99–109.

- 4 D. R. Crapper, S. S. Krishnan and S. Quittkat, *Brain*, 1976, **99**, 67–80.
- 5 T. Kiss, K. Gajda-Schranz and P. Zatta, *Neurodegenerative Diseases and Metal Ions*, Wiley & Sons, Chichester, 2006.
- 6 A. L. Florence, A. Gauthier, R. J. Ward and R. R. Crichton, *Neurodegeneration*, 1995, **4**, 449–455.
- 7 G. J. Kontoghiorghes and A. Kolnagou, *Curr. Med. Chem.*, 2005, **12**, 2695–2709.
- 8 G. J. Kontoghiorghes, *Lancet*, 1985, **1**, 817.
- 9 M. Y. Moridani, G. S. Tilbrook, H. H. Khodr and R. C. Hider, *J. Pharm. Pharmacol.*, 2002, **54**, 349–364.
- 10 M. A. Santos, M. Gil, L. Gano and S. Chaves, *JBIC, J. Biol. Inorg. Chem.*, 2005, **10**, 564–580.
- 11 D. E. Green, C. L. Ferreira, R. V. Stick, B. O. Patrick, M. J. Adam and C. Orvig, *Bioconjugate Chem.*, 2005, **16**, 1597–1609.
- 12 S. Piyamongkol, T. Zhou, Z. D. Liu, H. H. Khodr and R. C. Hider, *Tetrahedron Lett.*, 2005, **46**, 1333–1336.
- 13 R. Grazina, L. Gano, J. Sebestik and M. A. Santos, *J. Inorg. Biochem.*, 2008, **103**, 262–273.
- 14 M. A. Santos, S. Gama, L. Gano, G. Cantinho and E. Farkas, *Dalton Trans.*, 2004, 3772–3781.
- 15 M. A. Santos, *Coord. Chem. Rev.*, 2008, **252**, 1213–1224.
- 16 S. Gama, M. Gil, L. Gano, E. Farkas and M. A. Santos, *J. Inorg. Biochem.*, 2009, **103**, 288–298.
- 17 M. A. Santos, S. Gama, L. Gano and E. Farkas, *J. Inorg. Biochem.*, 2005, **99**, 1845–1852.
- 18 E. T. Clarke and A. E. Martell, *Inorg. Chim. Acta*, 1992, **191**, 57–63.
- 19 A. E. Martell, R. M. Smith and R. J. Motekaitis, *Critically Selected Stability Constants of Metal Complexes Database*, 1997, College Station TX.
- 20 E. Farkas, E. A. Enyedy and H. Csoka, *Polyhedron*, 1999, **18**, 2391–2398.
- 21 Z. D. Liu and R. C. Hider, *Coord. Chem. Rev.*, 2002, **232**, 151–171.
- 22 W. R. Harris and V. L. Pecoraro, *Biochemistry*, 1983, **22**, 292–299.
- 23 R. J. Motekaitis and A. E. Martell, *Inorg. Chim. Acta*, 1991, **183**, 71–80.
- 24 W. R. Harris and J. Sheldon, *Inorg. Chem.*, 1990, **29**, 119–124.
- 25 G. Serratrice, J.-B. Galey, E. S. Aman and J. Dumats, *Eur. J. Inorg. Chem.*, 2001, 471–479.
- 26 W. R. Harris and A. E. Martell, *Inorg. Chem.*, 1976, **15**, 713–720.
- 27 S. Gama, M. Gil, L. Gano, E. Farkas and M. A. Santos, *Coadjuvation of a bis(3-hydroxy-4-pyridinone) with a Deferriprone Derivative*, John Libbey Eurotext, Paris, 2006.
- 28 M. A. Santos, S. Gama, M. Gil and L. Gano, *Hemoglobin*, 2008, **32**, 1–10.
- 29 E. T. Clarke and A. E. Martell, *Inorg. Chim. Acta*, 1992, **196**, 185–194.
- 30 M. A. Santos, M. Gil, S. Marques, L. Gano, G. Cantinho and S. Chaves, *J. Inorg. Biochem.*, 2002, **92**, 43–54.
- 31 L. Zékány and I. Nagypál, *Computational Methods for the Determination of Stability Constants*, ed. D. J. Leggett, Plenum Press, New York, 1985.
- 32 W. H. Armstrong, M. E. Roth and S. J. Lippard, *J. Am. Chem. Soc.*, 1987, **109**, 6318–6326.
- 33 M. Gerloch, J. Lewis, F. E. Mabbs and A. Richards, *J. Chem. Soc. A*, 1968, 112–116.
- 34 J. C. Cobas, F. J. Sardina and S. Dominguez, *MestReC*, 2004, Santiago de Compostela.
- 35 O. Coskuner and E. A. A. Jarvis, *J. Phys. Chem. A*, 2008, **112**, 2628–2633.
- 36 G. G. Surpateanu, F. Delattre, P. Woisel, G. Vergoten and G. Surpateanu, *J. Mol. Struct.*, 2003, **645**, 29–36.
- 37 G. G. Surpateanu, G. Vergoten and G. Surpateanu, *J. Mol. Struct.*, 2000, **526**, 143–150.
- 38 G. G. Surpateanu, G. Vergoten and G. Surpateanu, *J. Mol. Struct.*, 2001, **559**, 263–271.
- 39 F. A. CAChe Group, *Fujitsu CAChe Worksystem software*, 15244 NW Greenbrier Parkway, Beaverton, OR 97006-5764, USA.
- 40 M. J. Frisch, G. W. Trucks, H. B. Schlegel, G. E. Scuseria, M. A. Robb, J. R. Cheeseman, J. A. Montgomery, Jr., T. Vreven, K. N. Kudin, J. C. Burant, J. M. Millam, S. S. Iyengar, J. Tomasi, V. Barone, B. Mennucci, M. Cossi, G. Scalmani, N. Rega, G. A. Petersson, H. Nakatsuji, M. Hada, M. Ehara, K. Toyota, R. Fukuda, J. Hasegawa, M. Ishida, T. Nakajima, Y. Honda, O. Kitao, H. Nakai, M. Klene, X. Li, J. E. Knox, H. P. Hratchian, J. B. Cross, V. Bakken, C. Adamo, J. Jaramillo, R. Gomperts, R. E. Stratmann, O. Yazyev, A. J. Austin, R. Cammi, C. Pomelli, J. Ochterski, P. Y. Ayala, K. Morokuma, G. A. Voth, P. Salvador, J. J. Dannenberg, V. G. Zakrzewski, S. Dapprich, A. D. Daniels, M. C. Strain, O. Farkas, D. K. Malick, A. D. Rabuck, K. Raghavachari, J. B. Foresman, J. V. Ortiz, Q. Cui, A. G. Baboul, S. Clifford, J. Cioslowski, B. B. Stefanov, G. Liu, A. Liashenko, P. Piskorz, I. Komaromi, R. L. Martin, D. J. Fox, T. Keith, M. A. Al-Laham, C. Y. Peng, A. Nanayakkara, M. Challacombe, P. M. W. Gill, B. G. Johnson, W. Chen, M. W. Wong, C. Gonzalez and J. A. Pople, *GAUSSIAN 03 (Revision C.02)*, Gaussian, Inc., Wallingford, CT, 2004.
- 41 G. Faa and G. Crisponi, *Coord. Chem. Rev.*, 1999, **184**, 291–310.
- 42 G. Gran, *Acta Chem. Scand.*, 1950, **4**, 559–577.
- 43 H. M. Irving, M. G. Miles and L. D. Pettit, *Anal. Chim. Acta*, 1967, **38**, 475–488.
- 44 L. O. Ohman and W. Forsling, *Acta Chem. Scand.*, 1981, **35**, 795–802.
- 45 C. F. Baes and R. E. Mesmer, *The Hydrolysis of Cations*, Wiley, New York, 1976.
- 46 A. Sabatini and I. Bertini, *Inorg. Chem.*, 1965, **4**, 959–961.
- 47 P. Gans, A. Sabatini and A. Vacca, *Talanta*, 1996, **43**, 1739–1753.
- 48 A. K. Covington, M. Paabo, R. A. Robinson and R. G. Bates, *Anal. Chem.*, 1968, **40**, 700–706.
- 49 D. F. Evans, *J. Chem. Soc.*, 1959, 2003–2005.
- 50 E. N. Sloth and C. S. Garner, *J. Chem. Phys.*, 1954, **22**, 2064–2066.